HHS Public Access

Author manuscript

RSC Adv. Author manuscript; available in PMC 2017 September 29.

Published in final edited form as:

RSC Adv. 2016 ; 6(98): 95715–95721. doi:10.1039/C6RA21226C.

Paramagnetic relaxation enhancement for protein-observed ^{19}F NMR as an enabling approach for efficient fragment screening

Laura M.L. Hawk[a], **Clifford T. Gee**[a], **Andrew K. Urick**[a,b], **Haitao Hu**[b], and **William C.K. Pomerantz**[a]

[a]Department of Chemistry, University of Minnesota, 207 Pleasant St. SE, Minneapolis, MN 55455, United States

[b]Lilly Research Laboratories, Eli Lilly and Company, Lilly Corporate Center, Indianapolis, IN 46285, United States

Abstract

Protein-observed ^{19}F (PrOF) NMR is an emerging tool for ligand discovery. To optimize the efficiency of PrOF NMR experiments, paramagnetic relaxation enhancement through the addition of chelated Ni(II) was used to shorten longitudinal relaxation time without causing significant line broadening. Thus enhancing relaxation time leads to shorter experiments without perturbing the binding of low- or high-affinity ligands. This method allows for time-efficient screening of potential ligands for a wide variety of proteins in the growing field of fragment-based ligand discovery.

Graphical Abstract

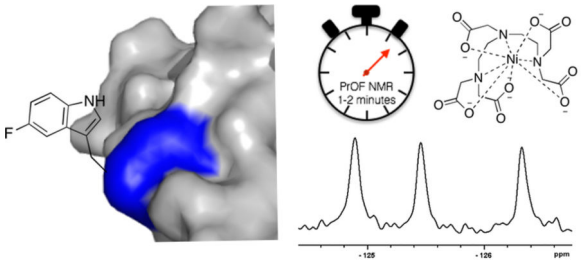

Introduction

Biomolecular NMR is a widespread tool for evaluating the structure and dynamics of biopolymers in isolation and in complexes. In the context of small molecule discovery, biomolecular NMR of proteins labelled with NMR active nuclei (e.g., ^{1}H-^{15}N HSQC NMR) has proven to be a valuable structure-based method for identifying binding sites and quantifying affinities of small molecule ligands.[1,2] New fast pulsing methods such as SOFAST-HMQC have decreased experiment time considerably; however, screening large compound libraries for protein binding by NMR can be a time- and material-intensive

Electronic Supplementary Information (ESI) available: [details of any supplementary information available should be included here]. See DOI: 10.1039/x0xx00000x

process.[3] We recently reported a protein-observed ^{19}F NMR (PrOF NMR) method for small molecule screening using a fluorine-labelled protein domain, KIX.[4] In that study, 508 small molecules were screened in mixtures of six requiring five minutes per experiment or 510 minutes of total experiment time and 20 mg of protein. Although this approach gives a modest time enhancement over SOFAST ^{1}H-^{15}N HMQC NMR on small to medium sized proteins,[5] the length and material consumption can still be limiting.

In NMR experiments, the recycle delay, during which the spectrometer is idle while the magnetization relaxes after a radio frequency pulse, comprises up to 80% or more of the total experiment time (Figure 1B).[6] Shorter recycle delays allow more scans per unit time, leading to more efficient instrument use. One strategy employed to shorten recycle delays is the addition of a paramagnetic metal to decrease the longitudinal relaxation time (T_1) of ^{1}H, ^{13}C, and ^{15}N nuclei in labelled proteins while minimizing unfavourable line-broadening from decreasing transverse relaxation time (T_2).[6–11] The application of paramagnetic additives to ^{19}F NMR has also been described in the context of NMR with molecular oxygen.[12] However, the specialized NMR tubes required would not be ideal for routine small molecule screening. These studies did not explore if the beneficial effects of paramagnetic metal additives are retained in the presence of bound ligands of varying affinity, a question we examine herein.

In this work, we explore the application of paramagnetic relaxation enhancement (PRE) to PrOF NMR, utilizing a solvent-accessible side-chain labelling scheme. This labelling scheme is well-suited to studying protein-protein interaction interfaces, which contain a high proportion of aromatic amino acids[13] that can readily be biosynthetically replaced with their fluorinated counterparts. The appended fluorine atoms on the side chains are more solvent exposed than backbone amides, and are potentially the most solvent exposed nuclei in a protein, allowing for access by paramagnetic additives in the bulk solvent. We demonstrate that PRE can reduce experiment times significantly by shortening the recycle delay with minimal line broadening from T_2 effects, ultimately leading to a marked enhancement in sensitivity. In the context of low-complexity molecules commonly used in fragment-based ligand discovery screening, we further show improvements by using this method for rapidly obtaining dissociation constants for weak-binding fragments. In addition to fragment screening, this method may also be useful for proteins available in limited abundance such as GPCRs,[14,15] as the signal to noise increases by the square root of the number of scans. Importantly, this approach is also compatible with proteins containing metal binding hexahistidine affinity tags and with various fluorinated amino acids.

NMR studies of fluorinated biomolecules have been applied to diverse biophysical processes, including protein folding and ligand binding.[16,17] The high sensitivity (83% that of proton), 100% natural abundance, absence of background in biological systems, and large chemical shift range all serve to make ^{19}F NMR an attractive tool for characterizing biological systems. Several recent studies have screened for ligand binding by PrOF NMR.[4,18–21] Although the ^{19}F NMR spectra can be readily acquired,[5] library screening by this method nevertheless requires a significant amount of experiment time. Shortened experiments would increase throughput in a small molecule NMR screen where the number of experiments may be large.

Results and Discussion

To find a metal that would shorten T_1 while minimally affecting T_2, the effects of several metals on ^{19}F T_1 and T_2 were compared. To minimize interactions between the metal and protein or small molecule, the metals were chelated, initially with the common chelator EDTA. For subsequent work we moved to DTPA, which forms a more stable metal chelate (Figure 1C).[22,23] We initially tested nickel, dysprosium, holmium, and thulium chelates to determine their effect on the relaxation properties of small molecule 4-fluorophenylalanine (4FF).[16,17] In addition to changing the sample's relaxation properties, the three lanthanides tested also cause lanthanide-induced shifts in the NMR spectrum, which have been utilized in 2D ^{1}H-^{1}H and ^{1}H-^{15}N systems to resolve resonance overlap.[23] Because of the environmental sensitivity of the ^{19}F nucleus, most PrOF NMR spectra of folded proteins show strong resonance dispersion and would not significantly benefit from lanthanide-induced shift reagents. Chelated Ni(II) showed the strongest effect on T_1 of the metals tested (Figure S1A), was the most economical, and did not introduce the additional complications of a shift reagent. Therefore, it was selected for further study.

To determine the optimal chelated Ni(II) concentration for protein studies, we explored the effect of a range of concentrations of chelated Ni(II) on the relaxation properties of 4FF (Figure S1A) as well as 5-fluoroindole (Figure S1B), the side chain present in proteins that have been ^{19}F-labelled at their tryptophan residues. The T_1 values of both of these molecules at Ni(II) concentrations up to 320 mM for 4FF and 200 mM for 5-fluoroindole were determined by inversion-recovery experiments. T_2^* values were determined from the peakwidth at half height. Because of the importance of peakwidth for resolving spectral resonances, T_2^* was used rather than T_2. For both 4FF and 5-fluoroindole, the highest Ni(II) concentration tested led to a more than a 100-fold decrease in T_1 values (Table 1). T_2^* also decreased with increasing chelated Ni(II) concentration, leading to approximately a 5-fold increase in peak width at 200 mM chelated Ni(II). Concentrations of 20–50 mM provide an optimal balance between T_1 reduction and T_2^* reduction and agree well with the 50 mM Ni(II) used by Cai et al. in ^{1}H, ^{15}N, and ^{13}C experiments.[6]

We then moved to testing the effects of Ni-DTPA on a model protein, the first domain of the bromodomain-containing protein Brd4, hereafter referred to as Brd4. Bromodomains are epigenetic regulatory domains, inhibition of which has therapeutic implications for cancer, heart disease, and inflammation[24,25] and are often targeted in fragment-screening campaigns.[26–28] For these studies, Brd4 was biosynthetically ^{19}F-labelled using the amino acid precursor 5-fluoroindole at all three tryptophan sites (W75, W81, and W120; Figure 1A) due to the enrichment of aromatic amino acids at protein-protein interaction interfaces.[13,29] When small molecules or ε-acetylated histone substrates bind to Brd4, we have observed a significant perturbation of the W81 resonance, which is located in the binding pocket. The resonance corresponding to W75, which is located beneath the binding pocket, experiences minor perturbations due to the environmental sensitivity of fluorine. The resonance corresponding to W120, which is located 36 Å from the binding site, generally shows minimal perturbation. T_1 measurements were carried out on 5-fluorotryptophan (5FW)-labelled Brd4 solutions titrated with Ni-DTPA without significantly affecting resonance width (Figure S2).

As expected, increasing concentrations of Ni-DTPA led to decreases in the T_1 (Table 1; Figure S3). The T_1 of the fluorine appended to W120 decreases the most rapidly and continues decreasing as more Ni-DTPA is added, suggesting that this fluorine is most accessible to the paramagnetic additive (80% reduction in T_1 at 20 mM Ni-DTPA), with W81 being intermediate in accessibility (75% reduction). The fluorine on W75 (50% reduction) is least accessible, and its T_1 value is less affected by Ni-DTPA. While the level of accessibility to paramagnetic additives consistent with T_1 measurements differs from the level of solvent exposure determined by the program GetArea,[30] the accessibility of the appended fluorine atom may differ from that of the residue as a whole. The extent of T_1 reduction upon addition of Ni-DTPA correlates with the apparent solvent exposure of the 5-position of the indole ring of the labelled tryptophans (Figure S4). These results are consistent with solvent accessible nuclei experiencing the strongest PRE effects.

The fluorines appended to W75 and W81 reach their T_1 minima at 20 mM metal; doubling the metal concentration to 40 mM had little effect on T_1 values. Therefore, 20 mM Ni-DTPA was used for further experiments to minimize the Q-damping effects resulting from additional ions in solution and concomitant loss of sensitivity.[31]

In the absence of Ni-DTPA, experiments were carried out with a recycle delay of 1 second (1.2 times the measured T_1 value of W81, the residue most affected by ligand binding in the binding pocket), with a total experiment time of five minutes (280 scans) at modest protein concentrations of 50 μM. With 20 mM Ni-DTPA present, the recycle delay was shortened to 0.24 seconds for a consistent value of 1.2 times the measured T_1 of W81. In this case, the experiment time was reduced to two minutes (350 scans) at the same protein concentration with similar signal-to-noise for the W81 resonance (11.8 with Ni-DTPA vs. 10.9 without), a 60% reduction in experiment time (Figure 2). The signal-to-noise ratio may be further improved if Q-damping effects could be mitigated. The T_1 value of W120 (0.15 sec) is more reduced than that of W81 (0.20 sec) by the addition of 20 mM Ni-DTPA. Consequently, the relative intensity of W120 increases with the addition of 20 mM Ni-DTPA because the net magnetization has more fully relaxed back to the ground state before application of the next pulse. In contrast, W75 has a longer T_1 value (0.27 sec) than W81 and thus its resonance is truncated by the short recycle delay of this experiment. Because W75 is farther from the binding pocket, the experiment was optimized for maximizing signal-to-noise per unit time of W81. Because binding sites must be accessible to their binding partners, amino acid side chains located at protein-protein interaction interfaces should also be accessible to paramagnetic additives and thus subject to substantial PRE effects, allowing for shortened recycle at delays and experiment times.

The chemical shift of W75 of Brd4 resonance is slightly perturbed upon titration of Ni-DTPA, moving 0.04 ppm in the presence of 20 mM Ni-DTPA and 0.07 ppm in the presence of 40 mM Ni-DTPA, which are above the threshold for significance of 0.03 ppm.[19] However, binding is non-specific and the change in chemical shift does not reach a saturation point up to 200 mM Ni-DTPA (Figure S5). Similarly, the chemical shift of fluorine resonances can change substantially upon titration of deuterated solvent, underscoring the large environmental sensitivity of the fluorine nucleus.[32] Protein stability does not undergo large perturbations upon titration of Ni-DTPA, as measured by differential

scanning fluorimetry, a thermal shift assay. Changes in melting temperature were ≤1.2 °C by this method (Figure S6). To assess the functional effect of Ni-DTPA on binding, fluorescence anisotropy was used to quantitate the binding affinity between a fluorescently labelled BET bromodomain ligand BI-BODIPY[19,33] and Brd4 (Figure S7). Binding was minimally perturbed, with only minor perturbations to the dissociation constant upon increasing concentrations of Ni-DTPA (Table S1). These results reduce concerns over the perturbing nature of the paramagnetic additive.

Having optimized conditions for running a time-efficient NMR experiment on a fluorinated protein, we next evaluated the time-enhancement effects of these conditions on ligand binding of both fragments and potent molecules. To this end, we tested two Brd4 inhibitors, compounds **1** and **2** (Figure 3A), uncovered in our small molecule discovery NMR fragment screens. Both **1** and **2** bind to 5FW-Brd4 (Figure 3B). For molecules like **1** and **2** that bind in the fast exchange regime, K_d values can be obtained by plotting changes in chemical shift against ligand concentration and fitting the resulting data to a binding isotherm that accounts for ligand depletion.[16] For both fragments, the resonance for W81 was the most perturbed, W75 was slightly perturbed, and W120 remained unaffected (Figure 3C and D). Fitting of the data for **1** to a binding isotherm yielded a K_d value of 81 ± 8 μM in the absence of paramagnetic metal and 87 ± 9 μM in the presence of 20 mM Ni-DPTA based on the chemical shift perturbation of W81. For **2**, the K_d values were 390 ± 60 μM without paramagnetic additive and 440 ± 30 μM with 20 mM Ni-DTPA. Additional bromodomain ligands were shown to bind to 5FW-Brd4 in the presence and absence of Ni-DTPA (Figure S8). These experiments were acquired at a higher magnetic field strength (564 MHz) allowing for a one-minute experiment time. We conclude that moderate concentrations of Ni-DTPA minimally perturb the binding of low-affinity molecules to this fluorinated protein and can thus be applied for fragment-based screens.

An experimental time reduction to one to two minutes allows for facile K_d determinations of fragments. Affinity determinations are valuable in fragment screening for prioritizing hits. We found that because low-affinity fragments have a short residence time on the protein, the ^{19}F-labelled residues are subject to PRE effects similar to those in the absence of fragment, allowing a full titration (nine samples) to be carried out in less than 20 minutes of experiment time. Without the advantage of pulse sequences like those used for 2D heteronuclear experiments such as SOFAST-HMQC which result in seven minute experiment times for similar sized proteins,[5,34] these ^{19}F experiments represent some of the fastest PrOF NMR experiments at the modest concentrations used.

We next sought to determine whether this method was compatible with more potent binders with longer residence times on the protein. We previously showed ^{19}F NMR spectra of 5FW-Brd4 exhibit slow exchange kinetics with known ligand (+)-JQ1 (K_d = 77 nM),[35] consistent with a long residence time on the protein. In our hands, the spectra acquired with one equivalent of (+)-JQ1 are qualitatively similar in the presence and absence of Ni-DTPA (Figure S9). However, the presence of this tight binding ligand limits the interaction of the paramagnetic additive and the labelled residue. Therefore, the T_1 experiences a smaller reduction in the presence of (+)-JQ1, consistent the r^{-6} distance dependence of relaxation times as described by the Solomon-Bloembergen equations.[6] Despite the changes of T_1

values, the W81 resonance is similarly perturbed by (+)-JQ1 in the presence and absence of Ni-DTPA, and spectra remain consistent with a tight-binding molecule in slow exchange.

Finally, to assess the generality of using PRE to shorten PrOF NMR experiments, we tested the compatibility of Ni-DTPA with three additional ^{19}F-labelled protein constructs. We tested proteins with hexahistidine affinity tags due to their ability to chelate metals. Encouragingly, spectra of hexahistidine-tagged 5FW-Brd4 recorded in the presence of 40 mM Ni-DTPA had linewidths similar to those of 5FW-Brd4 without its affinity tag, indicating that the Ni-DTPA is compatible with the presence of a hexahistidine tag despite this sequence's high affinity for Ni(II) (Figure S10). Ni-DTPA was also tested and is compatible with 3-fluorotyrosine (3FY)-labelled Brd4 (Figure S11) and 3FY-labelled KIX (Figure S12). Because 3FY KIX shows larger perturbations in its NMR spectrum than 5FW Brd4 upon addition of Ni-DPTA, the capacity of KIX for binding small molecules in the presence of Ni-DTPA was tested by both fluorescence anisotropy and PrOF NMR. Fluorescence anisotropy showed a small but significant dose-dependent increase in the K_d of the interaction between a fluorescein-labelled peptide of the transcriptional activation domain of MLL and the KIX protein at increasing concentrations of Ni-DPTA (Figure S13 and Table S2). For 20 mM Ni-DTPA, the increases in K_d were within two-fold. Using PrOF NMR, the K_d measured for the binding of KIX ligand Naphthol-AS-E phosphate[36] in the presence of 20 mM Ni-DTPA was 187 ± 50 μM, similar to the previously reported K_d of 115 ± 15 μM (Figure S14).[18]

In addition to the proteins studied here, Cai et al. also measured PRE effects on the ^{15}N-labeled protein SUMO-1 using a DO2A (1,7-dicarboxymethyl-1,4,7,10-tetraazacyclododecane) chelator for Ni(II) rather than DTPA.[6] PRE effects from chelated Ni(II) have been also been applied to ^{13}C-ribosome nascent chains.[10] Finally, the ^{13}C, ^{15}N-labelled intrinsically disordered protein α-synuclein, which is known to bind metals, has also been subjected to PRE conditions with chelated Ni(III) with minimal changes observed in its spectra.[7] These results support a broader use with proteins.

Conclusions

We were able to shorten T_1 times of our ^{19}F- labelled proteins without significantly changing resonance width by adding Ni-DTPA. The T_1 time of each residue was reduced by at least 50%, with the actual value depending on residue accessibility to the paramagnetic additive. The T_1 of the binding site residue was reduced by ~75%. By shortening the recycle delay based on these T_1 times, experiment time decreases 60% while conserving the signal-to-noise ratio of the binding site residue. The addition of Ni-DTPA does not significantly perturb ligand binding, making it a useful additive for shortening the total time for screening compounds by PrOF NMR and obtaining dissociation constants by ligand titration. For fragment screening, a two minute experiment would allow for ~700 mixtures of small molecules to be screened in 24 h of spectral acquisition time. Using six molecules per mixture, this affords libraries of over 4000 compounds to be tested in a day for a protein target of this size. Additional gains in sensitivity may be possible by using neutral Ni(II) chelates.[6,7,37] Other metals may also have favourable properties. Fe(III) has shown promise in some experiments,[38] although T_2 effects may be too substantial for PrOF NMR

experiments.[39] In addition to efficient screening of large compound libraries, this method can reduce protein concentration needs, or allow for the use of non-cryogenically cooled NMR probes for PrOF NMR screening.

Experimental

General NMR methods

Unless otherwise noted, spectra were acquired on a 500 MHz Bruker Avance III HD equipped with a 5 mM Prodigy TCI cryoprobe at 25°C. All experiments were performed in 50 mM Tris, 100 mM NaCl at pH 7.4 with 5% D_2O added for lock. Spectra were referenced to TFA at −76.55 ppm. All processing was done using TopSpin.

T_1 and T_2^* determination

Inversion-recovery experiments were carried out with 100 μM 5FW Brd4 or 5 mM small molecule (4-fluorophenylalanine and 5-fluoroindole). T_2* measurements for small molecules were taken on a 500 MHz Bruker Avance III with a BBFO probe. ^{19}F NMR spectra were acquired at 470 MHz. The 90° pulsewidth was calibrated for each experiment. Variable delay values ranged from 50 msec to 8 seconds, with the small molecules requiring 4 transients and the protein 40–80 transients. The recycle delay time was set to at least five times the measured T_1 value. T_2* values were determined by measuring the peakwidth at half height of the ^1H-decoupled ^{19}F resonances for small molecules and undecoupled ^{19}F resonances for proteins. Peakwidth was converted to T_2* using the equation $T_2^* = 1/(\pi^*\text{peakwidth})$.

PrOF NMR experiments

Experiments were carried out with 50 μM 5FW Brd4. Spectra were taken with a spectral width of 10 ppm, acquisition time of 0.05 seconds, and calibrated pulsewidths. Recycle delays were 1 second in the absence of Ni-DTPA and 0.24 seconds with 20 or 40 mM Ni-DTPA. JQ1 was added from a 10 mM stock solution in ethylene glycol. Fragments were added from 100 mM stock solutions in DMSO. Napththol-AS-E-phosphate was added from a solution of 40 mM DMSO. Line broadening of 10 Hz was applied during processing. Spectra of 5FW Brd4 with compounds **3** and **4** were taken on a 600 MHz Bruker Avance III spectrometer with a quadruple resonance HFCN CryoProbe. ^{19}F NMR spectra were acquired at 564 MHz. Changes in chemical shift upon titration of small molecules was fit to equation 1 to determine K_d, where $[L]_0$ and $[P]_0$ are the total concentrations of ligand and protein, respectively, Δ_{obs} is the observed change in chemical shift, and Δ_{max} is the maximum change in chemical shift.

$$\Delta_{\text{obs}}=\Delta_{\text{max}}\frac{K_d+[L]_0+[P]_0-\sqrt{(K_d+[L]_0+[P]_0)^2-4[P]_0[L]_0}}{2[P]_0} \quad (1)$$

Synthesis of DTPA-chelated metals

Metal (Ho(III)Cl_3•$6H_2O$ (Sigma Aldrich), Ni(II)SO_4•$6H_2O$ (Alfa Aesar), DyI_3 (Sigma Aldrich), or $TmCl_3$ (Sigma Aldrich)) was dissolved to 0.25 mM in H_2O with two equivalents of DTPA. The pH was raised with NaOH until all the DTPA went into solution (pH ~7). The reaction was stirred for an additional two hours. At this point, a xylenol orange test was negative for free metal.[40] Water was removed by lyophilization and the complex was resuspended at 0.5 to 1 M in H_2O for use in NMR experiments.

Protein expression and purification

5FW Brd4, was expressed and purified as previously described.[41] Briefly, *E. coli* containing plasmids for both pRARE with a chloramphenicol resistance selectable gene and Brd4 in a pNIC-BSA2 plasmid with a kanamycin selectable gene were cultured in LB containing 100 mg/L kanamycin and 35 mg/L chloramphenicol at 37 °C, then pelleted by centrifugation and resuspended in defined media containing 60 mg/L 5-fluoroindole and no tryptophan. 3FY Brd4 and 3FY KIX were expressed in a similar manner, but with unlabelled tryptophan and 80 mg/L 3-fluorotyrosine in place of tyrosine. For all proteins, after a 60-minute recovery period, the culture was cooled to 20 °C and expression was induced with 1 mM IPTG. The bacterial pellet was lysed with sonication and purified on a Ni-NTA affinity column, eluted with an imidazole gradient. The hexahistidine tag was removed by cleavage with TEV protease. After buffer exchange, the protein was stored in 50 mM Tris, 100 mM NaCl, pH 7.4.

Differential scanning fluorimetry

Differential scanning fluorimetry was performed on a CFX384 Real-Time PCR Detection System (BioRad). Purified unlabelled Brd4 (18 μM final concentration in 50 mM phosphate buffer (pH 7.4) with 150 mM NaCl) was assayed, in replicates of 12, in a 384-well plate with increasing Ni-DTPA concentrations. SYPRO Orange Protein Gel Stain (1:5000; Sigma-Aldrich) was used as the fluorescent probe at 5× concentration. Protein stability was investigated using 0.5 °C increments and 15 s incubations per increment from 24 to 99 °C. The inflection point of the transition curve/melting temperature (T_m) was calculated using the Boltzmann equation within the Protein Thermal Shift Software (v.1.1; Applied Biosystems).

Fluorescence anisotropy

Fluorescence anisotropy experiments were performed to quantitate the binding of BI-BODIPY[33] and unlabelled Brd4 as well as Fl-MLL[18] and unlabelled KIX. Emission and excitation were measured at 485 and 535 nm, respectively, on a Tecan Infinite 500 in a 384-well plate (Corning 4511). All experiments were carried out in triplicate, with at least two independent measurements. Data were fit in GraphPad Prism 6. K_d values were determined from equation 2, where c is the maximum anisotropy level, b is the minimum anisotropy value, and $[L]_0$ and $[P]_0$ have the same meanings as equation 1.

$$y=c+(b-c)\frac{K_d+[L]_0+[P]_0-\sqrt{(K_d+[L]_0+[P]_0)^2-4[L]_0[P]_0}}{2a} \quad (2)$$

Supplementary Material

Refer to Web version on PubMed Central for supplementary material.

Acknowledgments

This work was supported by the NSF CAREER award (CHE-1352019) and NIH training grants 5T32GM008347-23 (A.K.U.) and T32-GM08700 (C.T.G.).

References

1. Shuker SB, Hajduk PJ, Meadows RP, Fesik SW. Science. 1996; 274:1531–1534. [PubMed: 8929414]
2. Vogtherr, M., Fiebig, K. Modern Methods of Drug Discovery. Basel: Birkhäuser Basel; 2003. p. 183-202.
3. Pellecchia M, Bertini I, Cowburn D, Dalvit C, Giralt E, Jahnke W, James TL, Homans SW, Kessler H, Luchinat C, Meyer B, Oschkinat H, Peng J, Schwalbe H, Siegal G. Nat Rev Drug Discov. 2008; 7:738–745. [PubMed: 19172689]
4. Gee CT, Koleski EJ, Pomerantz WCK. Angew. Chem. Int. Ed. Engl. 2015; 54:3735–3739. [PubMed: 25651535]
5. Harner MJ, Chauder BA, Phan J, Fesik SW. J. Med. Chem. 2014; 57:9687–9692. [PubMed: 25314628]
6. Cai S, Seu C, Kovacs Z, Sherry AD, Chen Y. J. Am. Chem. Soc. 2006; 128:13474–13478. [PubMed: 17031960]
7. Theillet F-X, Binolfi A, Liokatis S, Verzini S, Selenko P. J Biomol NMR. 2011; 51:487–495. [PubMed: 22008951]
8. Yamamoto K, Vivekanandan S, Ramamoorthy A. J Phys Chem B. 2011; 115:12448–12455. [PubMed: 21939237]
9. Eletsky A, Moreira O, Kovacs H, Pervushin K. J Biomol NMR. 2003; 26:167–179. [PubMed: 12766412]
10. Chan SHS, Waudby CA, Cassaignau AME, Cabrita LD, Christodoulou J. J Biomol NMR. 2015; 63:151–163. [PubMed: 26253948]
11. Takeuchi K, Frueh DP, Hyberts SG, Sun Z-YJ, Wagner G. J. Am. Chem. Soc. 2010; 132:2945–2951. [PubMed: 20155902]
12. Kitevski-LeBlanc JL, Evanics F, Prosser RS. J Biomol NMR. 2009; 45:255–264. [PubMed: 19655092]
13. Bogan AA, Thorn KS. J. Mol. Biol. 1998; 280:1–9. [PubMed: 9653027]
14. Liu JJ, Horst R, Katritch V, Stevens RC, Wüthrich K. Science. 2012; 335:1106–1110. [PubMed: 22267580]
15. Manglik A, Kim TH, Masureel M, Altenbach C, Yang Z, Hilger D, Lerch MT, Kobilka TS, Thian FS, Hubbell WL, Prosser RS, Kobilka BK. Cell. 2015; 161:1101–1111. [PubMed: 25981665]
16. Arntson KE, Pomerantz WCK. J. Med. Chem. 2015
17. Marsh ENG, Suzuki Y. ACS Chem. Biol. 2014; 9:1242–1250. [PubMed: 24762032]
18. Pomerantz WC, Wang N, Lipinski AK, Wang R, Cierpicki T, Mapp AK. ACS Chem. Biol. 2012; 7:1345–1350. [PubMed: 22725662]
19. Urick AK, Hawk LML, Cassel MK, Mishra NK, Liu S, Adhikari N, Zhang W, Dos Santos CO, Hall JL, Pomerantz WC. ACS Chem. Biol. 2015; 10:2246–2256. [PubMed: 26158404]

20. Ge X, MacRaild CA, Devine SM, Debono CO, Wang G, Scammells PJ, Scanlon MJ, Anders RF, Foley M, Norton RS. J. Med. Chem. 2014; 57:6419–6427. [PubMed: 25068708]
21. Leung EWW, Yagi H, Harjani JR, Mulcair MD, Scanlon MJ, Baell JB, Norton RS. Chem Biol Drug Des. 2014; 84:616–625. [PubMed: 24813479]
22. Nash KL, Brigham D, Shehee TC, Martin A. Dalton Trans. 2012; 41:14547–14556. [PubMed: 23080218]
23. Sattler M, Fesik SW. J. Am. Chem. Soc. 1997
24. Prinjha RK, Witherington J, Lee K. Trends Pharmacol Sci. 2012; 33:146–153. [PubMed: 22277300]
25. Nicodeme E, Jeffrey KL, Schaefer U, Beinke S, Dewell S, Chung C-W, Chandwani R, Marazzi I, Wilson P, Coste H, White J, Kirilovsky J, Rice CM, Lora JM, Prinjha RK, Lee K, Tarakhovsky A. Nature. 2010; 468:1119–1123. [PubMed: 21068722]
26. Martin LJ, Koegl M, Bader G, Cockcroft X-L, Fedorov O, Fiegen D, Gerstberger T, Hofmann MH, Hohmann AF, Kessler D, Knapp S, Knesl P, Kornigg S, Muller S, Nar H, Rogers C, Rumpel K, Schaaf O, Steurer S, Tallant C, Vakoc CR, Zeeb M, Zoephel A, Pearson M, Boehmelt G, McConnell D. J. Med. Chem. 2016; 59:4462–4475. [PubMed: 26914985]
27. Taylor AM, Côté A, Hewitt MC, Pastor R, Leblanc Y, Nasveschuk CG, Romero FA, Crawford TD, Cantone N, Jayaram H, Setser J, Murray J, Beresini MH, de Leon Boenig G, Chen Z, Conery AR, Cummings RT, Dakin LA, Flynn EM, Huang OW, Kaufman S, Keller PJ, Kiefer JR, Lai T, Li Y, Liao J, Liu W, Lu H, Pardo E, Tsui V, Wang J, Wang Y, Xu Z, Yan F, Yu D, Zawadzke L, Zhu X, Zhu X, Sims RJ, Cochran AG, Bellon S, Audia JE, Magnuson S, Albrecht BK. ACS Med Chem Lett. 2016; 7:531–536. [PubMed: 27190605]
28. Yu J-L, Chen T-T, Zhou C, Lian F-L, Tang X-L, Wen Y, Shen J-K, Xu Y-C, Xiong B, Zhang N-X. Acta Pharmacol. Sin. 2016; 37:984–993. [PubMed: 27238211]
29. Watkins AM, Arora PS. ACS Chem. Biol. 2014; 9:1747–1754. [PubMed: 24870802]
30. Fraczkiewicz R, Braun W. J. Comput. Chem. 1998; 19:319–333.
31. Kelly AE, Ou HD, Withers R, Dötsch V. J. Am. Chem. Soc. 2002; 124:12013–12019. [PubMed: 12358548]
32. Hansen PE, Dettman HD, Sykes BD. J. Magn. Reson. 1985; 62:487–496.
33. Zhang Z, Kwiatkowski N, Zeng H, Lim SM, Gray NS, Zhang W, Yang PL. Mol. BioSyst. 2012; 8:2523–2524. [PubMed: 22673640]
34. Harner MJ, Frank AO, Fesik SW. J Biomol NMR. 2013; 56:65–75. [PubMed: 23686385]
35. Mishra NK, Urick AK, Ember SWJ, Schönbrunn E, Pomerantz WC. ACS Chem. Biol. 2014; 9:2755–2760. [PubMed: 25290579]
36. Best JL, Amezcua CA, Mayr B, Flechner L, Murawsky CM, Emerson B, Zor T, Gardner KH, Montminy M. Proc Natl Acad Sci USA. 2004; 101:17622–17627. [PubMed: 15585582]
37. Voehler MW, Collier G, Young JK, Stone MP, Germann MW. J. Magn. Reson. 2006; 183:102–109. [PubMed: 16949320]
38. Kislukhin AA, Xu H, Adams SR, Narsinh KH, Tsien RY, Ahrens ET. Nature Mater. 2016; 15:662–668. [PubMed: 26974409]
39. Jiang Z-X, Feng Y, Yu YB. Chem. Commun. (Camb.). 2011; 47:7233–7235. [PubMed: 21617807]
40. Averill DJ, Garcia J, Siriwardena-Mahanama BN, Vithanarachchi SM, Allen MJ. Journal of Visualized Experiments : JoVE. 2011
41. Gee CT, Arntson KE, Urick AK, Mishra NK, Hawk LML, Wisniewski AJ, Pomerantz WCK. Nat. Protoc. 2016; 11:1414–1427. [PubMed: 27414758]

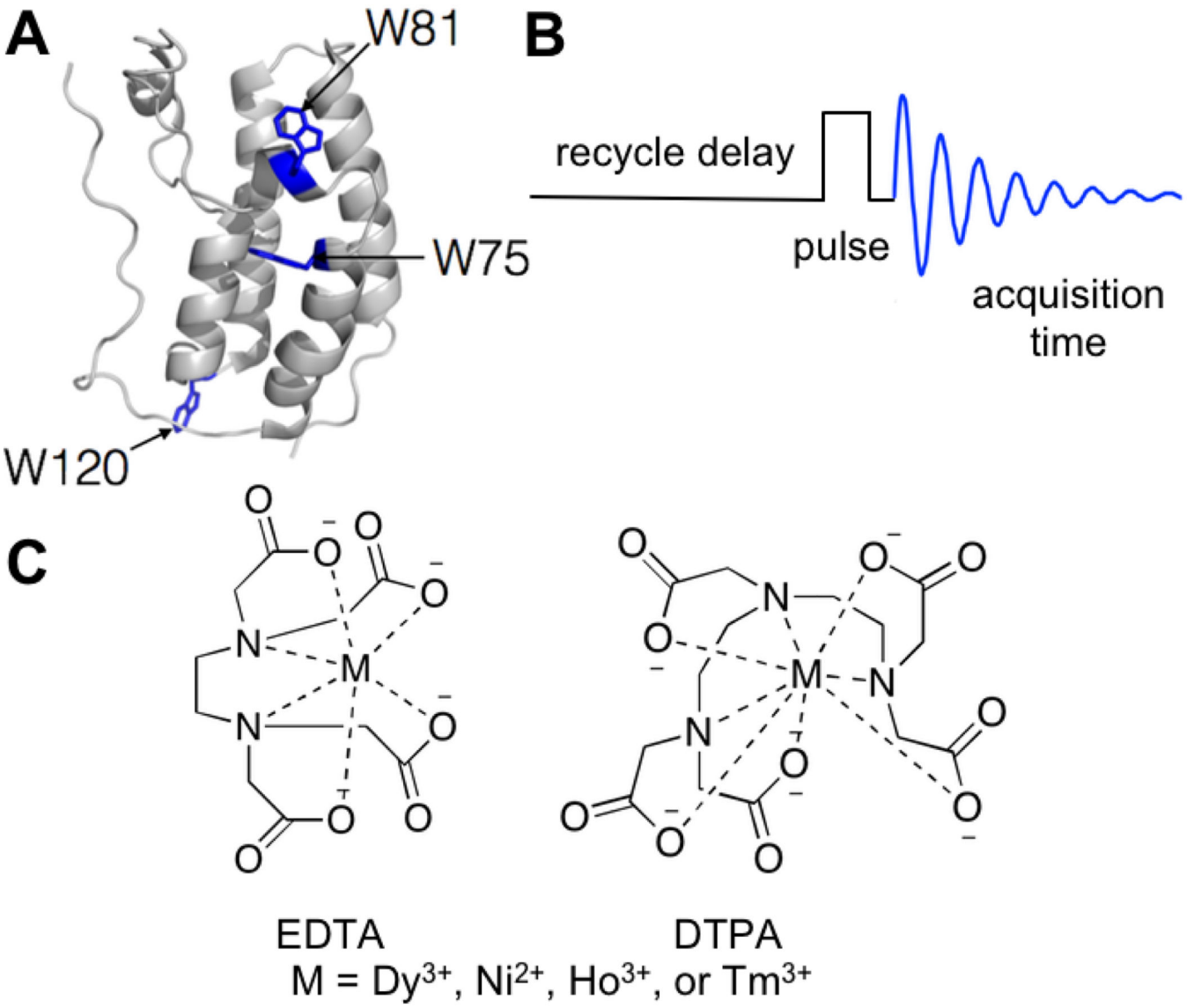

Figure 1.

A. Brd4 with sites of fluorine-labelled tryptophans highlighted in blue. B. Standard 1D ^{19}F NMR pulse sequence with 90° pulse. C. Structures of EDTA and DTPA chelates used in these experiments.

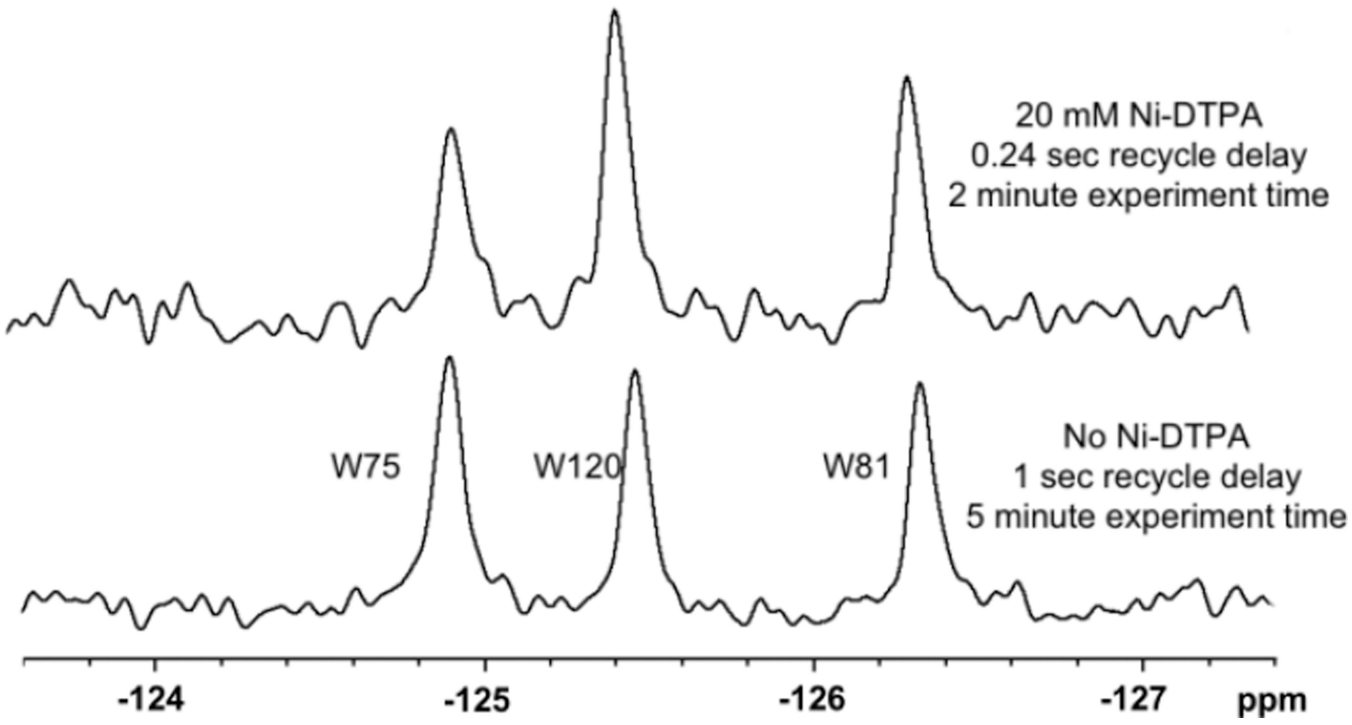

Figure 2.

Comparison of ^{19}F NMR spectra of 50 μM 5FW-Brd4 in the presence and absence of paramagnetic additive. The addition of 20 mM Ni-DTPA allows a 60% reduction in experiment time while preserving the signal-to-noise ratio of W81, perturbations of which report on ligand binding. The signal-to-noise ratio of W81 without Ni-DTPA was 11.8, and with Ni-DTPA was 10.9.

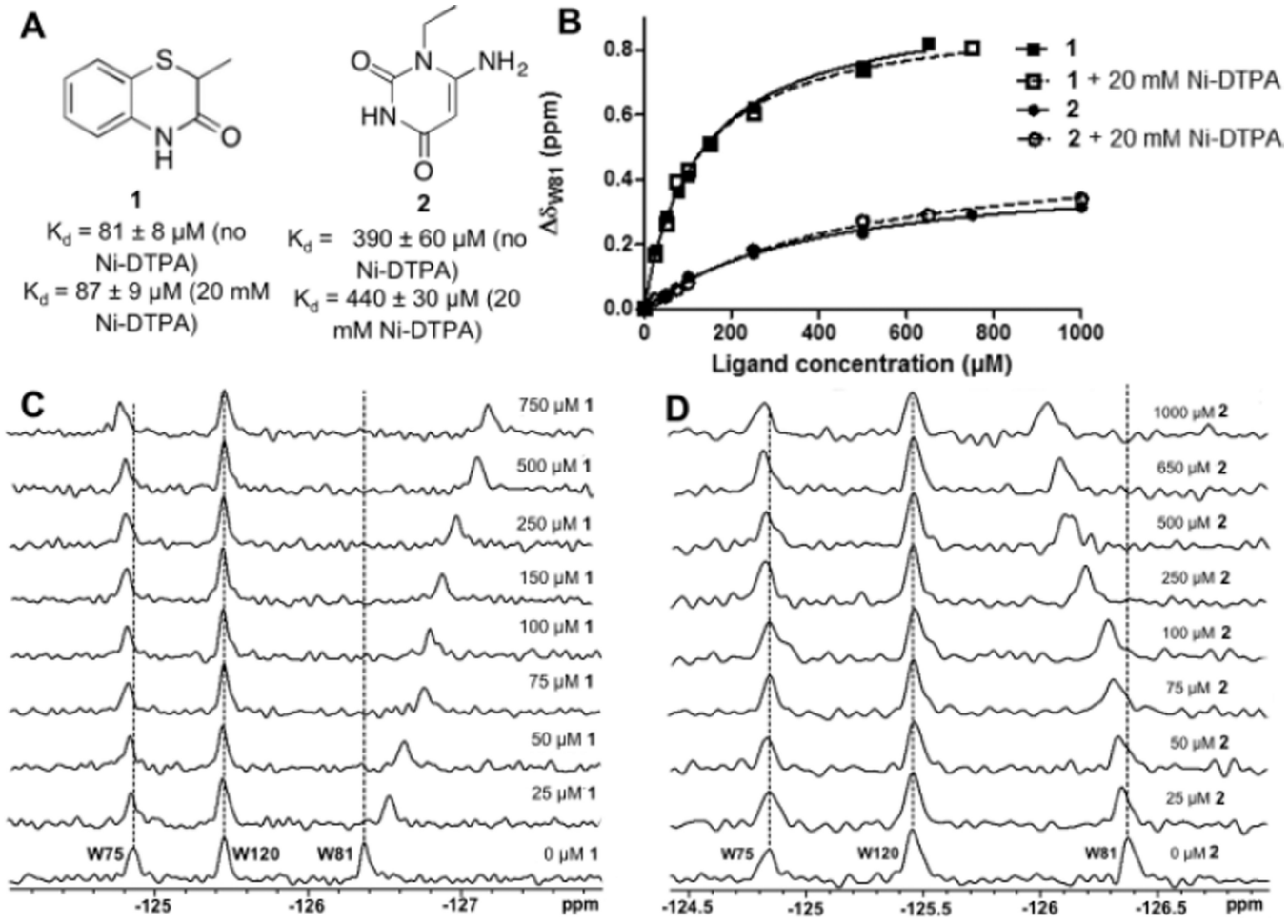

Figure 3.

A. Compounds **1** and **2** both bind 5FW Brd4 in the fast exchange regime. B. The binding isotherms showing the change in chemical shift of W81 upon titration of **1** and **2**. Solid lines with filled symbols show the isotherms in the absence of Ni-DTPA; dashed lines with unfilled symbols indicate the presence of 20 mM Ni-DTPA. C,D. **1** and **2** were titrated into 50 μM 5FW Brd4, leading to a dose-dependent change in the chemical shift of the resonance corresponding to W81, located in the binding site.

Table 1

T_1 and T_2^* values for fluorine resonances of small molecules and protein Brd4 at increasing Ni(II) concentrations

Compound	Ni-DTPA (mM)	T_1 (msec)	T_2* (msec)
5-fluoroindole	0	4890	208
	20	528	107
	50	202	80
4FF	0	1870	77
	20	216	97
	40	113	80
W75 (+ JQ1)	0	508 (552)	7.5 (7.1)
	20	269 (399)	7.2 (6.2)
	40	294 (346)	6.4 (6.9)
W120 (+ JQ1)	0	721 (685)	8.4 (6.1)
	20	146 (212)	8.0 (7.2)
	40	86 (156)	8.4 (8.1)
W81 (+ JQ1)	0	837 (772)	8.8 (7.0)
	20	196 (289)	8.6 (5.4)
	40	192 (149)	8.6 (2.9)

Small molecules used in this study were 5-fluoroindole and 4-fluorophenylalanine (4FF). T_1 and T_2* values were also measured for 5-fluorotryptophan residues within the protein Brd4 with and without the addition of Brd4 ligand, JQ1, that binds near W81.